HNUE JOURNAL OF SCIENCE DOI: 10.18173/2354-1059.2021-0031
Natural Sciences 2021, Volume 66, Issue 2, pp. 83-99
This paper is available online at http://stdb.hnue.edu.vn

STUDY ON ELASTIC PROPERTY OF STAINLESS STEEL UNDER PRESSURE

Nguyen Quang Hoc[1], Nguyen Duc Hien[2], Trinh Duc Nam[1] and Vu Long Thanh[1]
[1]*Faculty of Physics, Hanoi National University of Education*
[2]*Mac Dinh Chi High School, Chu Pah District, Gia Lai Province*

Abstract. The paper presents analytic expressions of the Helmholtz free energy and characteristic elastic deformation quantities such as the elastic moduli *E, K,* G and the elastic constants C_{11}, C_{12}, C_{44} for BCC interstitial and substitutional alloy with four components are determined by the statistical moment method. The obtained elastic quantities depend on temperature, pressure, the concentration of interstitial atoms, and the concentration of substitutional atoms. This is the elastic deformation theory of BCC interstitial and substitutional alloy with four components published for the first time. The elastic deformation theories of BCC metal, BCC binary interstitial alloy, BCC binary substitutional alloy, and BCC ternary interstitial and substitutional alloy are limit cases of the elastic deformation theory of BCC substitutional and interstitial alloy with four components. Our numerical calculations of the obtained theoretical results for metal Fe and alloy FeSi are in good agreement with other calculations and experiments. Other numerical calculations for alloys FeCr, FeNi, FeCrSi, FeNiSi, FeCrNiSi (some atoms Fe are substituted by atoms Cr and some other atoms Fe are substituted by atoms Ni) called stainless steels predict and orient experimental results in the future. Our numerical calculations for alloy FeCrNiSi are published for the first time.

Keywords: substitutional and interstitial alloy with four components, elastic moduli, elastic constants, stainless steels, statistical moment method.

1. Introduction

The FeCr binary system is the basis for a large class of important engineering materials known as stainless steel. Stainless steels combine good corrosion resistance with attractive mechanical properties. Some other properties of FeCr alloys are also of interest such as spin glass formation, sluggish formation of the σ phase, and strong swelling resistance in an irradiative medium. Phase equilibria and thermodynamic properties in the FeCr system have been reviewed comprehensively based on experimental information

Received May 9, 2021. Revised June 21, 2021. Accepted June 28, 2021.
Contact Nguyen Quang Hoc, e-mail address: hocnq@hnue.edu.vn

and available computer simulations. The evaluated phase equilibria show significant differences from the currently accepted thermodynamic description by the CALPHAD approach [1].

Iron and its alloys are widely used in structural, electrical, and other technological applications; thus, it is vital to have accurate values of iron's basic physical properties. Among physical properties, the elastic constants are of both fundamental and practical interests. Basic properties such as the bulk, shear, and Young's moduli can be calculated from the monocrystal elastic constants. Information on the influences of pressure and temperature on the elastic moduli and related aggregate properties of single crystals plays an essential role in predicting and understanding the interatomic interactions, strength, mechanical stability, phase transition mechanisms, and dynamical response of materials.

There are some theoretical research results on the elastic deformation of iron for example using the full-potential linear response linear-muffin-tin orbital (LMTO) method [2]. In this work, Sha and Cohen [2006] have performed a first-principles quasiharmonic lattice dynamics study to examine the elastic moduli of bcc Fe with pressures and temperatures.

Elastic deformation of iron and iron alloys is considered in many experiments. Resonant ultrasound spectroscopy was used to measure the monocrystal elastic constants of iron over a temperature range of 3 - 500 K [3]. The Young's modulus (E) and shear modulus (G) of isotropic Fe and binary Fe-C, Fe-Co, Fe-Cr, Fe-Ir, Fe-Mn, Fe-Ni, Fe-Pt, Fe-Re, Fe-Rh, and Fe-Ru alloys have been determined as functions of composition (0 to 10 at. pct) and temperature (77 to 473 K) by a pulse-echo technique (100 kHz elastic waves). The temperature dependence of E and G of the alloys is similar to that of iron, decreasing in a nonlinear manner from 77 to 473 K [4].

For geologists, Earth's core consists of an abundant source of pure iron and iron alloys while the mantle has silicate minerals [5]. Iron silicides have attracted a lot of attention in recent decades, due to their unusual physical properties and functional applications [6]. The distribution of the Si-atoms in alloy FeCrSi is discussed in comparison with some common transition metal silicide structures [7]. The electronic and thermodynamic properties of iron silicides such as B2-FeSi have been investigated using the first-principles method based on the plane-wave basis set in the ranges of 0 - 2400 K and 0 - 140 GPa [6]. Zhang et *al.* (2020) use a combination of first-principles calculation with special quasi-random structure and quasi-harmonic approximation methods to calculate the formation energy, mechanical and thermodynamic properties of binary FeCr and ternary FeCrSi random alloys [8]. A new FeCrSi base alloy that offers promise for improved corrosion resistance at a lower cost than state of the art FeCrAl and stainless steel alloys are reported [9]. The analytic expressions of the free energy, the mean nearest neighbor distance between two atoms, the elastic moduli, and the elastic constants for BCC substitution alloy AB with interstitial atom C under pressure are derived from the statistical moment method (SMM) [10-13]. The numerical results for alloy FeCrSi are compared with the numerical results for main metal Fe, substitution alloy FeCr, interstitial alloy FeSi, and experiments [14].

In this report, we present the theory of elastic deformation for body-centered cubic (BCC) substitutional and interstitial alloy with four components under pressure built by

the statistical moment method (SMM). Our numerical calculations of the obtained theoretical results are performed for metal Fe and alloys FeSi, FeCr, FeNi, FeCrSi, FeNiSi, FeCrNiSi (some atoms Fe are substituted by atoms Cr and some other atoms Fe are substituted by atoms Ni) called stainless steels

2. Content

2.1. Theory of elastic deformation for BCC substitutional and interstitial alloy AB_1B_2C under pressure

In our previous papers [10, 14, 15], we derived the analytic expressions of the cohesive energy u_0 and the alloy parameters $k, \gamma_1, \gamma_2, \gamma$ for the atom C in face center of cubic unit cell, the atom A_1 in the body center of the cubic unit cell, and the atom A_2 in peaks of the cubic unit cell for the BCC interstitial alloy AC in the approximation of two and three coordination spheres. In these papers, we also determined the cohesive energy and the metal parameters for atom A in the clean metal A in the approximation of two coordination spheres

If we know the form of the interaction potential between two atoms X (X = A, A1, A2, C), from the equation of state for alloy AC, we can find the nearest neighbor distance between two $r_{01X}(P,0)$ and the alloy parameters $k_X(P,0), \gamma_1(P,0), \gamma_2(P,0), \gamma(P,0)$ for atom X at temperature 0 K and pressure P. From that, we can determine the displacement $y_X(P,T)$ of atom X from the equilibrium position [10, 15], the nearest neighbor distance $r_{1X}(P,T)$ and the mean nearest neighbor distance $\overline{r_{1A}(P,T)}$ between two atoms A in the alloy AC.

The mean nearest neighbor distance between two atoms A in the BCC interstitial and substitutional alloy AB_1B_2C at pressure P and temperature T is calculated by

$$a_{AB_1B_2C} = c_{AC}a_{AC}\frac{B_{TAC}}{\overline{B_T}} + c_{B_1}a_{B_1}\frac{B_{TB_1}}{\overline{B_T}} + c_{B_2}a_{B_2}\frac{B_{TB_2}}{\overline{B_T}},$$

$$\overline{B_T} = c_{AC}B_{TAC} + c_{B_1}B_{TB_1} + c_{B_2}B_{TB_2}, c_{AC} = c_A + c_C,$$

$$a_{ABC} \equiv \overline{r_{1A}^{ABC}(P,T)}, a_{AC} \equiv \overline{r_{1A}^{AC}(P,T)}, a_B \equiv r_{1B}(P,T),$$

$$B_{TAC} = \frac{1}{\chi_{TAC}} = \frac{2P + \frac{3\sqrt{3}}{4a_{AC}}\frac{1}{3N}\left(\frac{\partial^2\psi_{AC}}{\partial a_{AC}^2}\right)_T}{3\left(\frac{a_{AC}}{a_{0AC}}\right)^3}, B_{TB_1} = \frac{1}{\chi_{TB_1}} = \frac{2P + \frac{3\sqrt{3}}{4a_{B_1}}\frac{1}{3N}\left(\frac{\partial^2\psi_{B_1}}{\partial a_{B_1}^2}\right)_T}{3\left(\frac{a_{B_1}}{a_{0B_1}}\right)^3},$$

$$B_{TB_2} = \frac{1}{\chi_{TB_2}} = \frac{2P + \frac{3\sqrt{3}}{4a_{B_2}}\frac{1}{3N}\left(\frac{\partial^2\psi_{B_2}}{\partial a_{B_2}^2}\right)_T}{3\left(\frac{a_{B_2}}{a_{0B_2}}\right)^3}, \quad (1)$$

$$\left(\frac{\partial^2\psi_{AC}}{\partial a_{AC}^2}\right)_T \approx (1-7c_C)\left(\frac{\partial^2\psi_A}{\partial a_A^2}\right)_T + c_C\left(\frac{\partial^2\psi_C}{\partial a_C^2}\right)_T + 2c_C\left(\frac{\partial^2\psi_{A_1}}{\partial a_{A_1}^2}\right)_T + 4c_C\left(\frac{\partial^2\psi_{A_2}}{\partial a_{A_2}^2}\right)_T,$$

$$\frac{1}{3N}\left(\frac{\partial^2\psi_X}{\partial a_X^2}\right)_T = \frac{1}{6}\frac{\partial^2 u_{0X}}{\partial a_X^2} + \frac{\hbar\omega_X}{4k_X}\left[\frac{\partial^2 k_X}{\partial a_X^2} - \frac{1}{2k_X}\left(\frac{\partial k_X}{\partial a_X}\right)^2\right], X = A, A_1, A_2, B_1, B_2, C.$$

The mean nearest neighbor distance between two atoms A in the BCC interstitial and substitutional alloy AB_1B_2C at pressure P and temperature 0 K is calculated by

$$a_{0AB_1B_2C} = c_{AC}a_{0AC}\frac{B_{0TAC}}{\overline{B_{0T}}} + c_{B_1}a_{0B_1}\frac{B_{0TB_1}}{\overline{B_{0T}}} + c_{B_2}a_{0B_2}\frac{B_{0TB_2}}{\overline{B_{0T}}}, \overline{B_{0T}} = c_{AC}B_{0TAC} + c_{B_1}B_{0TB_1} + c_{B_2}B_{0TB_2},$$
$$a_{0AB_1B_2C} \equiv \overline{r_{01A}^{AB_1B_2C}(P,0)}, a_{0AC} \equiv \overline{r_{01A}^{AC}(P,0)}, a_{0B_1} \equiv r_{01B_1}(P,0), a_{0B_2} \equiv r_{01B_2}(P,0). \quad (2)$$

The Helmholtz free energy of the BCC interstitial and substitutional alloy AB_1B_2C with the condition $c_C << c_{B_1}, c_{B_2} << c_A$ (c_A, c_{B_1}, c_{B_2} and c_C respectively are the concentrations of atoms A, B_1, B_2 and C) is equal to

$$\begin{aligned}
\psi_{AB_1B_2C} &= \left(1-c_{B_1}-c_{B_2}-7c_C\right)\psi_A + c_{B_1}\psi_{B_1} + c_{B_2}\psi_{B_2} + c_C\psi_C + 2c_C\psi_{A_1} + 4c_C\psi_{A_2} + TS_c^{AB_1B_2C} = \\
&= \left(1-7c_C\right)\psi_A + c_C\psi_C + 2c_C\psi_{A_1} + 4c_C\psi_{A_2} + TS_c^{AC} + c_{B_1}\left(\psi_{B_1}-\psi_A\right) + c_{B_2}\left(\psi_{B_2}-\psi_A\right) + \\
&+ TS_c^{AB_1B_2C} - TS_c^{AC} = \psi_{AC} + c_{B_1}\left(\psi_{B_1}-\psi_A\right) + c_{B_2}\left(\psi_{B_2}-\psi_A\right) + TS_c^{AB_1B_2C} - TS_c^{AC}, \\
\psi_{AC} &= \left(1-7c_C\right)\psi_A + c_C\psi_C + 2c_C\psi_{A_1} + 4c_C\psi_{A_2} - TS_c^{AC}, \\
\psi_X &\approx U_{0X} + \psi_{0X} + 3N\left\{\frac{\theta^2}{k_X^2}\left[\gamma_{2X}Y_X^2 - \frac{2\gamma_{1X}}{3}\left(1+\frac{Y_X}{2}\right)\right] + \right. \\
&\left. + \frac{2\theta^3}{k_X^4}\left[\frac{4}{3}\gamma_{2X}Y_X\left(1+\frac{Y_X}{2}\right) - 2\left[\gamma_{1X}^2 + 2\gamma_{1X}\gamma_{2X}\right]\left(1+\frac{Y_X}{2}\right)\left(1+Y_X\right)\right]\right\}, \\
\psi_{0X} &= 3N\theta\left[x_X + \ln\left(1-e^{-2x_X}\right)\right], Y_X \equiv x_X\coth x_X.
\end{aligned} \quad (3)$$

where ψ_X is the Helmholtz free energy of an atom X in clean material X, S_c^{AC} is the configurational entropy of the interstitial alloy AC and $S_c^{AB_1B_2C}$ is the configurational entropy of the interstitial and substitutional alloy AB_1B_2C.

The Young modulus of the alloy AB_1B_2C has the form

$$\begin{aligned}
E_{ABC} &= E_{AB} - \left(c_A + c_B\right)E_A + E_{AC} = c_B\left(E_B - E_A\right) + E_{AC}, \\
E_{AB_1B_2C} &= E_{AB_1} + E_{AB_2} - \left(c_A + c_{B_1} + c_{B_2}\right)E_A + E_{AC} = c_{B_1}\left(E_{B_1} - E_A\right) + c_{B_2}\left(E_{B_2} - E_A\right) + E_{AC}, \\
E_{AB_1} &= c_AE_A + c_{B_1}E_{B_1}, E_{AB_2} = c_AE_A + c_{B_2}E_{B_2}, \\
E_Z &= \frac{1}{\pi r_{1Z}A_{1Z}}, A_{1Z} = \frac{1}{k_Z}\left[1 + \frac{2\gamma_Z^2\theta^2}{k_Z^4}\left(1+\frac{1}{2}Y_Z\right)\left(1+Y_Z\right)\right], Y_Z \equiv x_Z\coth x_Z, \\
x_Z &= \frac{\hbar\omega_Z}{2\theta}, Z = A, B_1, B_2, E_{AC} = E_A\left(1 - 7c_C + c_C\frac{\frac{\partial^2\psi_C}{\partial\varepsilon^2} + 2\frac{\partial^2\psi_{A_1}}{\partial\varepsilon^2} + 4\frac{\partial^2\psi_{A_2}}{\partial\varepsilon^2}}{\frac{\partial^2\psi_A}{\partial\varepsilon^2}}\right), \\
\frac{\partial^2\psi_X}{\partial\varepsilon^2} &= \left\{\frac{1}{2}\frac{\partial^2U_{0X}}{\partial r_{1X}^2} + \frac{3}{4}\frac{\hbar\omega_X}{k_X}\left[\frac{\partial^2k_X}{\partial r_{1X}^2} - \frac{1}{2k_X}\left(\frac{\partial k_X}{\partial r_{1X}}\right)^2\right]\right\}.4r_{01X}^2 + \\
&+ \left(\frac{1}{2}\frac{\partial U_{0X}}{\partial r_{1X}} + \frac{3\theta Y_X}{2k_X}\frac{\partial k_X}{\partial r_{1X}}\right).2r_{01X}, x_X = \frac{\hbar\omega_X}{2\theta}, \omega_X = \sqrt{\frac{k_X}{m_X}}.
\end{aligned} \quad (4)$$

The bulk modulus of the alloy AB_1B_2C is

$$K_{AB_1B_2C} = \frac{E_{AB_1B_2C}}{3\left(1-2\nu_{AB_1B_2C}\right)}, \tag{5}$$

where $\nu_{AB_1B_2C}$ the Poisson ratio of the alloy AB_1B_2C.

The shearing modulus of the alloy AB_1B_2C is given by

$$G_{AB_1B_2C} = \frac{E_{AB_1B_2C}}{2\left(1+\nu_{AB_1B_2C}\right)}. \tag{6}$$

The elastic constants of the alloy AB_1B_2C are counted by

$$C_{11AB_1B_2C} = \frac{E_{AB_1B_2C}\left(1-\nu_{AB_1B_2C}\right)}{\left(1+\nu_{AB_1B_2C}\right)\left(1-2\nu_{AB_1B_2C}\right)}, \tag{7}$$

$$C_{12AB_1B_2C} = \frac{E_{AB_1B_2C}\nu_{AB_1B_2C}}{\left(1+\nu_{AB_1B_2C}\right)\left(1-2\nu_{AB_1B_2C}\right)}, \tag{8}$$

$$C_{44AB_1B_2C} = \frac{E_{AB_1B_2C}}{2\left(1+\nu_{AB_1B_2C}\right)}. \tag{9}$$

The Poisson ratio of the alloy AB_1B_2C is equal to

$$\nu_{AB_1B_2C} = c_A\nu_A + c_{B_1}\nu_{B_1} + c_{B_2}\nu_{B_2} + c_C\nu_C \approx c_A\nu_A + c_{B_1}\nu_{B_1} + c_{B_2}\nu_{B_2} \approx c_A\nu_A, \tag{10}$$

where $\nu_X\,(X = A, B_1, B_2, C)$ is the Poisson ratio of the material *X*.

When the concentration of interstitial atoms $c_C = 0,$ the theory of elastic deformation for above mentioned BCC substitutional and interstitial ternary alloy AB_1B_2C becomes the theory of elastic deformation for the BCC ternary substitutional alloy AB_1B_2. When the concentration of substitutional atoms $c_{B_1} = 0,$ the theory of elastic deformation for BCC substitutional and interstitial alloy AB_1B_2C becomes the theory of elastic deformation for the BCC ternary interstitial and substitutional alloy AB_2C. When the concentration of substitutional atoms $c_{B_2} = 0,$ the theory of elastic deformation for BCC substitutional and interstitial alloy AB_1B_2C becomes the theory of elastic deformation for the BCC ternary interstitial and substitutional alloy AB_1C. When the concentrations of substitutional atoms $c_{B_1} = c_{B_2} = 0,$ the theory of elastic deformation for BCC substitutional and interstitial alloy AB_1B_2C becomes the theory of elastic deformation for the BCC binary interstitial alloy AC. When the concentrations of substitutional atoms $c_{B_1} = c_{B_2} = 0$ and the concentration of interstitial atoms $c_C = 0,$ the theory of elastic deformation for BCC substitutional and interstitial alloy AB_1B_2C becomes the theory of elastic deformation for the BCC main metal A [15].

2.2. Numerical results and discussions for metal Fe and alloys FeCr, FeNi, FeSi, FeCrSi, FeNiSi, FeCrNiSi

In order to study alloys FeCr, FeNi, FeSi, FeCrSi, FeNiSi and FeCrNiSi, we use the Mie-Lennard-Jones (MLJ) pair interaction potential as follows [16]:

$$\varphi(r) = \frac{D}{n-m}\left[m\left(\frac{r_0}{r}\right)^n - n\left(\frac{r_0}{r}\right)^m \right], \tag{11}$$

where D is the depth of potential well corresponding to the equilibrium distance r_0, m and n are determined empirically. Then, the potential parameters for the interaction Fe-Si are determined by [17]

$$D_{\text{Fe-Si}} = \sqrt{D_{\text{Fe-Fe}} D_{\text{Si-Si}}}, r_{0\text{Fe-Si}} = \frac{1}{2}\left(r_{0\text{Fe-Fe}} + r_{0\text{Si-Si}}\right). \tag{12}$$

We find $m_{\text{Fe-Si}}$ and $n_{\text{Fe-Si}}$ by fitting the theoretical result with the experimental data for the Young modulus of interstitial alloy FeSi at room temperature. the potential parameters for the interactions Fe-Cr and Fe-Ni are determined analogically. The Mie-Lennard-Jones potential parameters for the interactions Fe-Fe, Cr-Cr, Ni-Ni, and Si-Si are given in Table 1. Here, we ignore the interactions Cr-Si, Ni-Si, and Cr-Ni.

Table 1. Mie-Lennard-Jones potential's parameters for interactions Fe-Fe, Cr-Cr, Ni-Ni and Si-Si

Interaction	D/k_B**(K)**	r_0 **(10^{-10} m)**	***m***	***n***
Fe-Fe [16]	4649.60	2.4775	7	11.5
Cr-Cr [16]	4792	2.4950	6	15.5
Ni-Ni [16]	4327.20	2.4780	8	9
Si-Si [16]	32701.70	2.2950	6	12

Our calculated results are summarised in tables from Table 2 to Table 16 and are illustrated in figures from Figure 1 to Figure 11. The comparison results are presented in Tables 4 and 5, and Tables 8-10.

Consider the case of FeCrNiSi when the concentrations $c_{\text{Cr}} = c_{\text{Ni}} = c_{\text{Si}} = 0$. Our calculated results for Fe in Tables 2 and 3 are similar to the results of Hoc and Hien (2018) [14]. The calculated results for the nearest neighbor distance, the elastic moduli, and the elastic constants for Fe at T = 300 K and P = 0 in [14] are in good agreement with experiments [18-20] and other calculations [20].

Table 2. Temperature dependence of elastic moduli for Fe at P = 0 from SMM

***T*(K)**	**100**	**300**	**500**	**700**	**1000**
$E(10^{10}\text{Pa})$	22.48	20.83	18.79	16.37	12.25
$K(10^{10}\text{Pa})$	15.61	14.47	13.05	11.37	6.50
$G(10^{10}\text{Pa})$	8.92	8.27	7.46	6.50	4.86

Table 3. Pressure dependence of nearest neighbor distance, relative change of volume, elastic moduli and elastic constants for Fe at T = 300 K from SMM

***P*(GPa)**	**10**	**30**	**50**	**70**
$r_1(10^{-10}\text{m})$	2.3797	2.3486	2.3247	2.3052
$\Delta V/V$	9.7	7.8	6.6	5.8
$E(10^{10}\text{Pa})$	3.19	4.11	4.98	5.82
$K(10^{10}\text{Pa})$	2.21	2.86	3.46	4.04
$C_{11}(10^{11}\text{Pa})$	3,90	5.03	6.09	7.12
$C_{12}(10^{11}\text{Pa})$	1.37	1.77	2.14	2.50
$C_{44}(10^{11}\text{Pa})$	1.26	1.63	1.98	2.31

Consider the case of FeCrNiSi when the concentrations $c_{\text{Ni}} = c_{\text{Si}} = 0$. Our calculated results for FeCr in Table 4 are similar to the results of Hoc and Hien (2018) [14].

Table 4. Dependences of elastic moduli and elastic constants on concentration of substitutional atoms Cr for FeCr at T = 300 K and P = 0

$c_{\text{Cr}}(\%)$	**3**	**6**	**9**	**12**	**15**
$E(10^{10}\text{Pa})$	20.91	20.99	21.08	21.17	21.25
$K(10^{10}\text{Pa})$	16.69	16.85	17.02	17.19	17.37
$C_{11}(10^{10}\text{Pa})$	27.50	27.68	27.89	28.09	28.30
$C_{12}(10^{10}\text{Pa})$	11.29	11.44	11.59	11.74	11.90
$C_{44}(10^{10}\text{Pa})$	8.09	8.12	8.15	8.17	8.20

Consider the case of FeCrNiSi when the concentrations $c_{\text{Ni}} = c_{\text{Cr}} = 0$. Our calculated results for FeSi at c_{Si} = 1% and T = 300 K in Table 5 are similar to the results of Hoc and Hien (2018) [14]. The calculated results for the lattice constant, the volume of unit cell and the bulk modulus for FeSi at c_{Si} = 1%, P = 0 and T = 300 K are in good agreement with experiments [5, 25], *ab initio* calculations [8, 22] and DFT calculations [22-25].

Table 5. Dependence of elastic moduli and elastic constants on pressure for FeSi at c_{Si} = 1% and T = 300 K

***P*(GPa)**	**10**	**30**	**50**	**70**
$E(10^{10}\text{Pa})$	33.93	54.01	72.53	90.22
$K(10^{10}\text{Pa})$	26.69	42.48	57.04	70.96
$C_{11}(10^{10}\text{Pa})$	44.26	70.43	94.58	117.65
$C_{12}(10^{10}\text{Pa})$	17.91	28.50	38.28	47.61
$C_{44}(10^{10}\text{Pa})$	13.17	20.96	28.15	35.02

Consider the case of FeCrNiSi when the concentration $c_{Ni} = 0$. Our calculated results for FeCrSi in figures from Figure 1 to Figure 4 are similar to the results of Hoc and Hien (2018) [14].

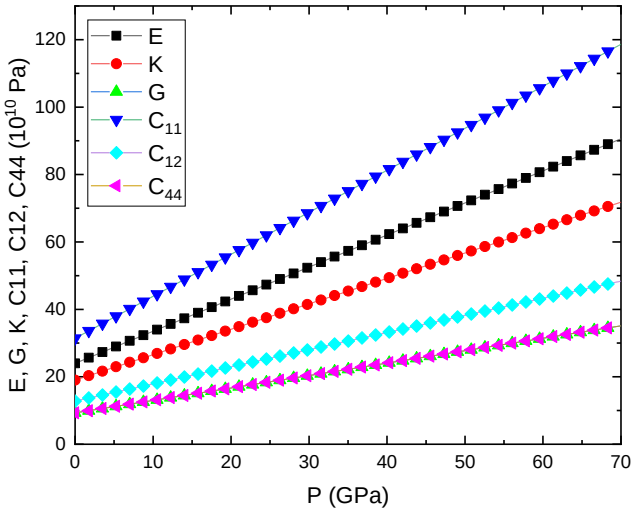

Figure 1. E(P), G(P), K(P),C_{11}(P), C_{12}(P), C_{44}(P) for FeCrSi at c_{Cr} = 4%, c_{Si} = 1%,T = 300 K

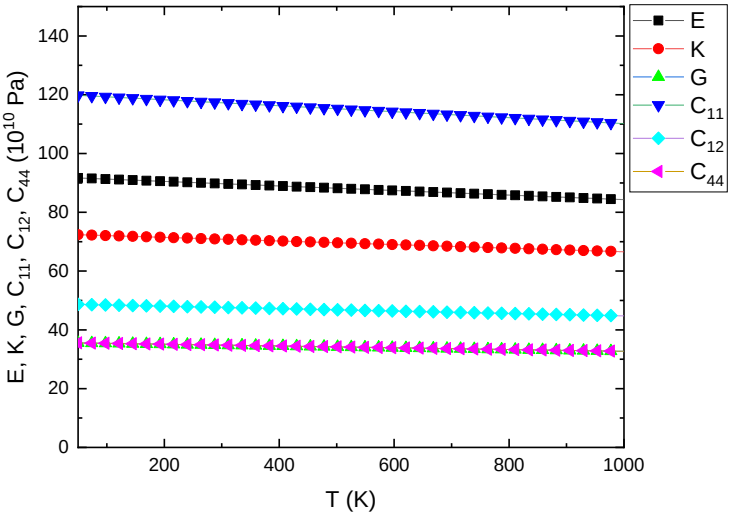

Figure 2. E(T), G(T), K(T), C_{11}(T), C_{12}(T), C_{44}(T) for FeCrSi at c_{Cr} = 4%, c_{Si} = 1%, P = 30 GPa

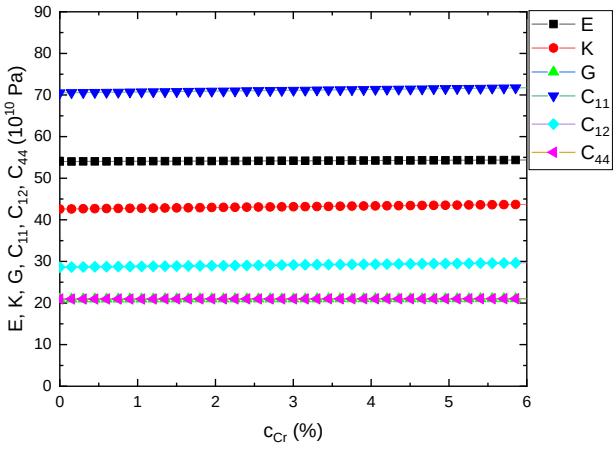

Figure 3. $E(c_{Cr})$, $G(c_{Cr})$, $K(c_{Cr})$, C_{11} (c_{Cr}), C_{12} (c_{Cr}), C_{44} (c_{Cr}) for FeCrSi at c_{Si} = 1%, P = 70 GPa, T = 300 K

For FeCrSi at the same pressure, the concentration of substitutional atoms Cr and the concentration of interstitial atoms Si when temperature increases, the mean nearest neighbor distance increases, the elastic moduli and the elastic constants decrease. For FeCrSi at the same temperature, the concentration of substitutional atoms Cr and the concentration of interstitial atoms Si when pressure increases, the mean nearest neighbor distance decreases, the elastic moduli, and the elastic constants increase. For FeCrSi at the same temperature, pressure, the concentration of substitutional atoms Cr when the concentration of interstitial atoms Si increases, the mean nearest neighbor distance increases, the elastic moduli, and the elastic constants increase. For FeCrSi at the same temperature, pressure, the concentration of interstitial atoms Si when the concentration of substitutional atoms Cr increases, the mean nearest neighbor distance decreases, the elastic moduli and the elastic constants decrease [14].

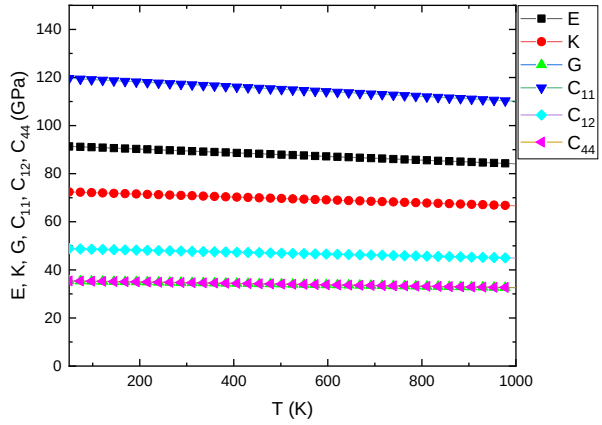

Figure 4. E(T), G(T), K(T), C_{11}(T), C_{12}(T), C_{44}(T) for FeCrSi at c_{Cr} = 4%, c_{Si} = 1%, P = 70 GPa

Consider the case of FeCrNiSi when the concentrations $c_{Cr} = c_{Si} = 0$. Our calculated results for FeNi are summarized in Table 6.

Table 6. Dependences of elastic moduli and elastic constants on concentration of substitutional atoms Ni for FeNi at T = 300 K and P = 0

c_{Ni}(%)	**3**	**6**	**9**	**12**	**15**
$E(10^{10}$Pa)	20.71	20.61	20.51	20.42	20.14
$K(10^{10}$Pa)	16.46	16.41	16.35	16.30	16.24
$C_{11}(10^{10}$Pa)	27.16	27.05	26.95	26.84	26.73
$C_{12}(10^{10}$Pa)	11.11	11.08	11.05	11.03	11.00
$C_{44}(10^{10}$Pa)	8.03	7.99	7.95	7.91	7.86

Consider the case of FeCrNiSi when the concentration $c_{Cr} = 0$. Our calculated results for FeNiSi are summarized in tables from Table 7 to Table 9 and illustrated in figures from Figure 5 to Figure 7.

Table 7. Dependence of elastic moduli and elastic constants on pressure for FeNiSi at c_{Ni} = 4%, c_{Si} = 1% and T = 300 K

***P*(GPa)**	**10**	**30**	**50**	**70**
$E(10^{10}$Pa)	33.79	53.80	72.26	89.89
$K(10^{10}$Pa)	26.68	42.48	57.05	70.97
$C_{11}(10^{10}$Pa)	44.15	70.31	94.42	117.46
$C_{12}(10^{10}$Pa)	17.94	28.56	38.36	47.72
$C_{44}(10^{10}$Pa)	13.11	20.87	28.03	34.87

Table 8. Dependence of elastic moduli and elastic constants on concentration of interstitial atoms Si for FeNiSi at c_{Ni} = 4%, P = 30 GPa and T = 300 K

c_{Si} **(%)**	**1**	**3**	**5**
$E(10^{10}$Pa)	53.80	72.22	90.64
$K(10^{10}$Pa)	42.48	56.01	69.07
$C_{11}(10^{10}$Pa)	70.31	93.48	116.23
$C_{12}(10^{10}$Pa)	28.56	37.28	45.49
$C_{44}(10^{10}$Pa)	20.87	28.10	35.37

Consider the case of FeCrNiSi. Our calculated results for this alloy with four components are summarized in Table 10 to Table 11 and illustrated in Figures 8 and 9.

Table 9. Dependence of elastic moduli and elastic constants on temperature for FeNiSi at c_{Ni} = 4%, c_{Si} = 1% and P = 70 GPa

***T*(K)**	**50**	**100**	**300**	**500**
$E(10^{10}\text{Pa})$	91.53	91.20	89.89	88.41
$K(10^{10}\text{Pa})$	72.26	72.01	70.97	69.81
$C_{11}(10^{10}\text{Pa})$	119.61	119.18	117.46	115.54
$C_{12}(10^{10}\text{Pa})$	48.59	48.42	47.7	46.94
$C_{44}(10^{10}\text{Pa})$	35.51	35.38	34.87	34.30

Table 10. Dependence of elastic moduli and elastic constants on pressure for FeCrNiSi at c_{Cr} = c_{Ni} = 2%, c_{Si} = 1% and T = 300 K

***P*(GPa)**	**10**	**30**	**50**	**70**
$E(10^{10}\text{Pa})$	33.88	53.81	72.18	89.74
$K(10^{10}\text{Pa})$	26.80	42.56	51.10	70.99
$C_{11}(10^{10}\text{Pa})$	44.32	70.38	101.60	117.39
$C_{12}(10^{10}\text{Pa})$	18.04	28.65	38.37	47.79
$C_{44}(10^{10}\text{Pa})$	13.14	20.87	27.99	34.03

Table 11. Dependence of elastic moduli and elastic constants on temperature for FeCrNiSi at c_{Ni} = 10%, c_{Si} = 1% and T = 300 K

***T*(K)**	**100**	**300**	**500**
$E(10^{10}\text{Pa})$	97.76	96.26	94.78
$K(10^{10}\text{Pa})$	77.28	76.22	75.05
$C_{11}(10^{10}\text{Pa})$	127.70	126.00	124.10
$C_{12}(10^{10}\text{Pa})$	52.05	51.34	50.54
$C_{44}(10^{10}\text{Pa})$	37.84	37.33	36.75

The dependences of the elastic moduli and the elastic constants on temperature, pressure, the concentration of substitutional atoms, and concentration of interstitial atoms for alloys FeNiSi and FeCrNiSi are similar to that for alloy FeCrSi.

Figure 10 is the pressure dependence of the Young modulus for alloys $FeNi_{4\%}$, $FeSi_{4\%}$, $FeCr_{4\%}Si_{1\%}$, $FeNi_{4\%}Si_{1\%}$, $FeCr_{2\%}Ni_{2\%}Si_{1\%}$ at T = 300 K. Figure 11 is the temperature dependence of the Young modulus for alloys $FeNi_{4\%}$, $FeSi_{4\%}$, $FeCr_{4\%}Si_{1\%}$, $FeNi_{4\%}Si_{1\%}$, $FeCr_{2\%}Ni_{2\%}Si_{1\%}$ at P = 30 GPa.

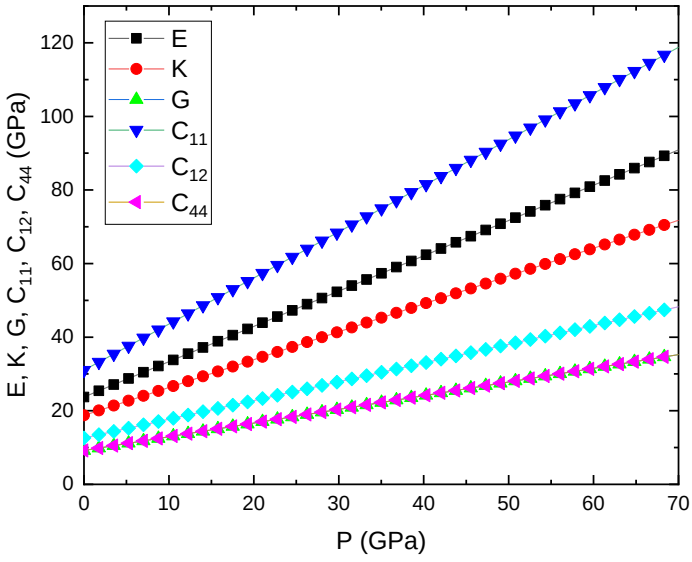

Figure 5. E(P), G(P), K(P), C_{11}(P), C_{12}(P), C_{44}(P) for FeNiSi at c_{Ni} = 4%, c_{Si} = 1%, T = 300 K

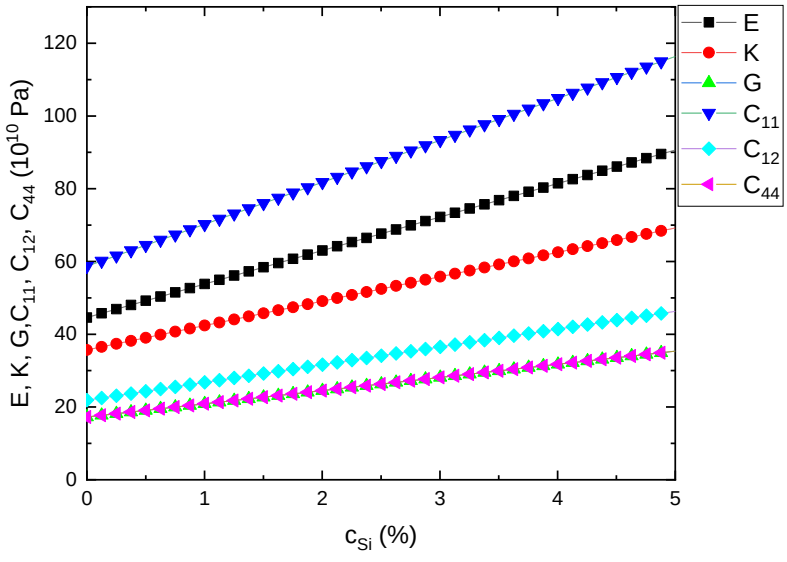

Figure 6. E(c_{Si}), G(c_{Si}), K(c_{Si}), C_{11}(c_{Si}), C_{12}(c_{Si}), C_{44}(c_{Si}) for FeNiSi at c_{Ni} = 4%, T = 300 K, P = 30 GPa

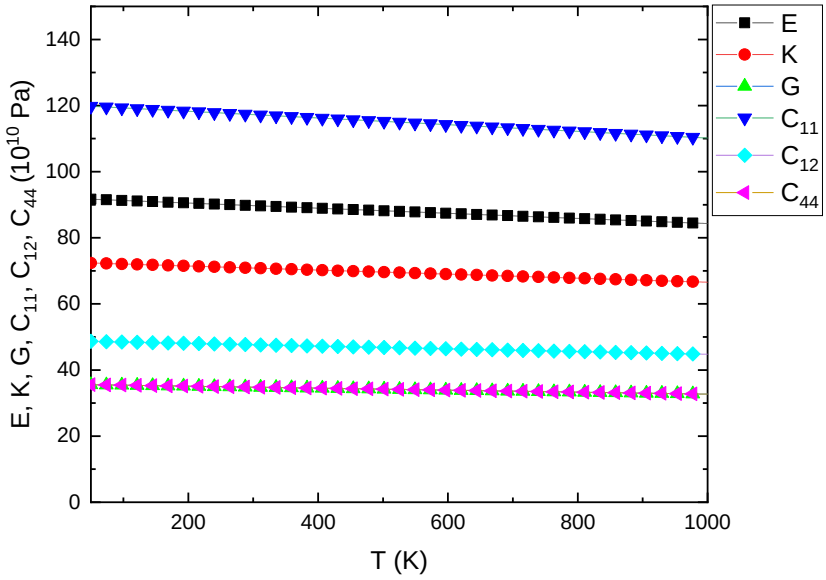

Figure 7. E(T), G(T), K(T), C_{11}(T), C_{12}(T), C_{44}(T) for FeNiSi at c_{Ni} = 4%, c_{Si} = 1%, P = 70 GPa

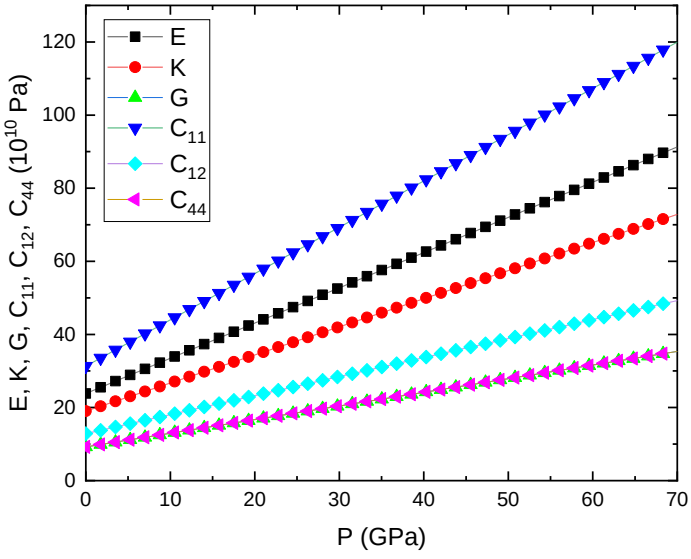

Figure 8. E(P), G(P), K(P), C_{11}(P), C_{12}(P), C_{44}(P) for FeCrNiSi at c_{Cr} = 2%, c_{Ni} = 2%, c_{Si} = 1%, T = 300 K

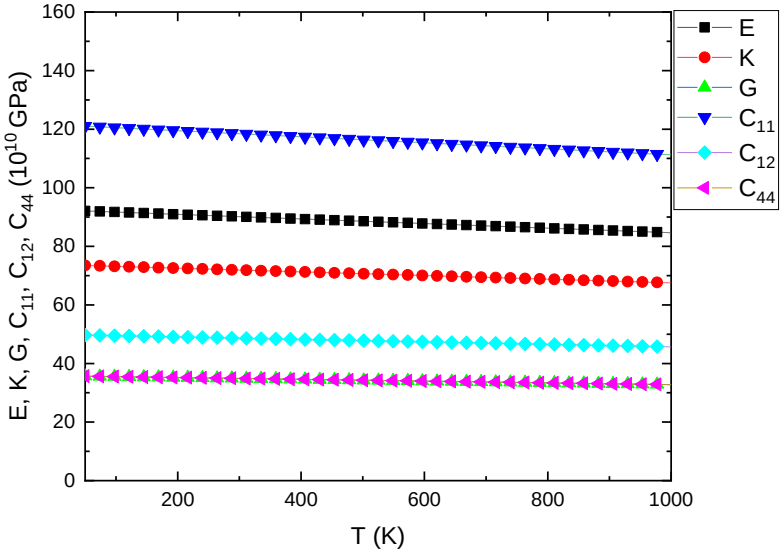

Figure 9. E(T), G(T), K(T), C_{11}(T), C_{12}(T), C_{44}(T) for FeCrNiSi at c_{Cr} = 2%, c_{Ni} = 2%, c_{Si} = 1%, P = 70 GPa

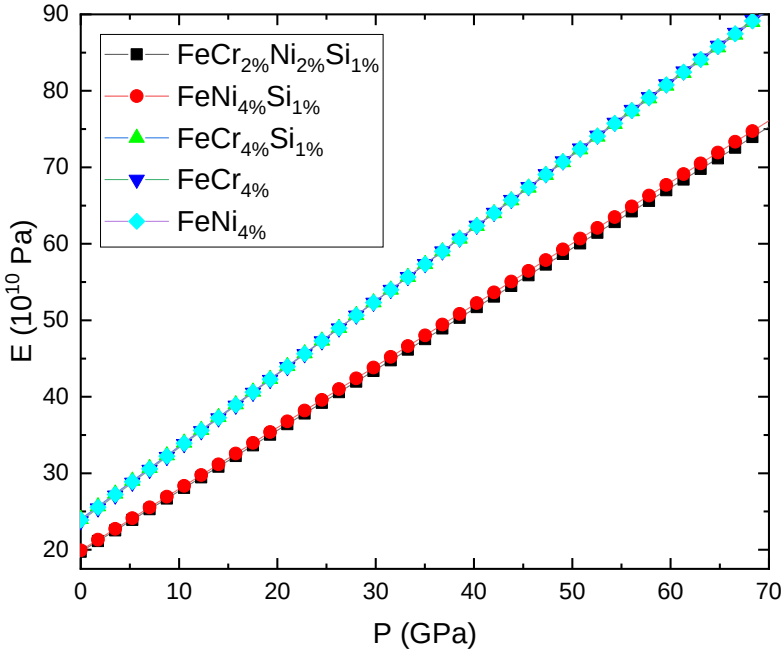

Figure 10. E(P) for $FeNi_{4\%}$, $FeSi_{4\%}$, $FeCr_{4\%}Si_{1\%}$, $FeNi_{4\%}Si_{1\%}$, $FeCr_{2\%}Ni_{2\%}Si_{1\%}$ at T = 300 K

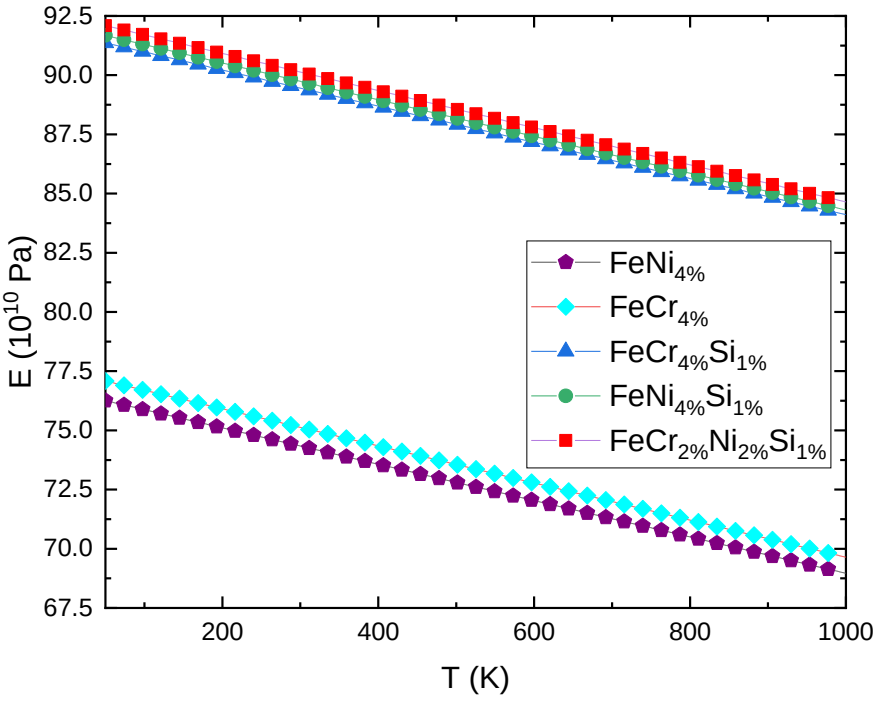

Figure 11. E(T) for $FeNi_{4\%}$,$FeSi_{4\%}$, $FeCr_{4\%}Si_{1\%}$, $FeNi_{4\%}Si_{1\%}$, $FeCr_{2\%}Ni_{2\%}Si_{1\%}$ at P = 30 GPa

3. Conclusions

The paper presents the theory of elastic deformation for BCC substitutional and interstitial alloy with four components at zero pressure and under pressure. The obtained elastic quantities depend on temperature, pressure, the concentration of substitutional atoms, and concentration of interstitial atoms. The elastic deformation theories of BCC metal, BCC binary interstitial alloy, BCC binary substitutional alloy, and BCC ternary interstitial and substitutional alloy are limit cases of the elastic deformation theory of BCC substitutional and interstitial alloy with four components. Our numerical calculations are carried out for alloys FeCr, FeNi, FeSi, FeCrSi, FeNiSi, FeCrNiSi, and metal Fe in the range of pressure from zero to 70 GPa, in the range of temperature from zero to 1000 K, in the range of concentration of substitutional atoms from zero to 15% and in the range of concentration of interstitial atoms from zero to 5%. Our calculated results for Fe and FeSi are compared with other calculations and experiments. Many of our new calculations predict and orient experimental results in the future.

REFERENCES

[1] W. Xiong, M. Selleby, Q. Chen, J. Osqvist and Y. Du, 2010. Phase equilibria and thermodynamic properties in the FeCr system. *Critical Review in Solid State and Materials Sciences,* Vol. 35, p. 215.

[2] X. Sha and R. E. Cohen, 2006. First-principles thermoelasticity of bcc iron under pressure. *Physical Review B,* Vol. 74, No. 21, p. 214111.

[3] D. G. Isaak and K. Masuda, 1995. Elastic and viscoelastic properties of α iron at high temperatures. *Journal of Geophysical Research: Solid Earth,* Vol. 100, No. B9, pp. 17689-17698.

[4] J. J. Adams, D. S. Agosta, D. S., R. G. Leisure and H. Ledbetter, 2006. Elastic constants of monocrystal iron from 3 to 500K. *Journal of Applied Physics.* Vol. 100, No. 11, p. 113530.

[5] S. Ono, T. Kikegawa and Y. Ohishi, 2007. Static compression of high-pressure phase FeSi. *European Journal of Mineral,* Vol. 19, pp. 183-187.

[6] K. M. Zhao, G. Jiang G and L. Wang, 2011. Electronic and thermodynamic properties of B2-FeSi from first principles. *Physica* B., Vol. 406, p. 363.

[7] B. I. Verkina and A. Ph. Prikhotko, 1983. Kriokristallu, Kiev (in Russian).

[8] J. Zhang, C. Su and Y. Liu, 2020. First-principle study of bcc Fe-Cr-Si binary and ternary random alloys from special quasi-random structure. *Physica B: Physics of Condensed Matter,* Vol. 586, p. 2085.

[9] M. P. Brady, K. Banta, J. Mizia, N. Lorenz, D. N. Leonard, Y. Yamamoto, M. DeFoort and J. R. Keizer,2017. Alloy corrosion considerations in low-cost, clean biomass cookstoves for the development world. *Energy for sustainable development*, Vol. 37, p. 20.

[10] N. Tang and V. V. Hung, 1988. Investigation of the thermodynamic properties of anharmonic crystals by the momentum method, (I) General results for FCC crystals. *Physica Status Solidi (b),* Vol. 149, p. 511.

[11] N. Tang and V. V. Hung, 1990. Investigation of the thermodynamic properties of anharmonic crystals by the momentum method, (II) Comparison of calculations with experiments for inert gas crystals. *Physica Status Solidi (b),* Vol. 161, p. 165.

[12] N. Tang and V. V. Hung, 1990. Investigation of the thermodynamic properties of anharmonic crystals by the momentum method, (III) Thermodynamic properties of the crystals at various pressures. *Physica Status Solidi (b),* Vol. 162, p. 371.

[13] N. Tang and V. V. Hung, 1990.Investigation of the thermodynamic properties of anharmonic crystals by the momentum method, (IV) The limiting of absolute stability and the melting temperature of crystals. *Physica Status Solidi (b),* Vol. 162, p. 379.

[14] N. Q. Hoc and N. D. Hien, 2018. Study on elastic deformation of substitution alloy AB with interstitrial atom C and BCC structure under pressure. *42nd Vietnam National Conference on Theoretical Physics (NCTP-42), IOP Conf. Series: Journal of Physics: Conf. Series,* Vol. 1034, p. 012005.

[15] V. V. Hung, 2009. *Statistical moment method in studying elastic and thermodynamic properties of crystals.* HNUE Publishing House, Hanoi.

[16] M. N. Magomedov, 1987. On calculating the Debye temperature and the Gruneisen parameter. *Zhurnal Fizicheskoi Khimii*, Vol. 61, No. 4, pp.1003-1009 (in Russian).

[17] R. J. Good and C. J. Hope, 1970. New combining rule for intermolecular distances in intermolecular potential functions. *The Journal of Chemical Physics*, Vol. 53, No. 2, pp. 540-543.

[18] D. R. Lide, 2005. *CRC Handbook of Chemistry and Physics*. Taylor & Francis, Boca Raton London, New York, Singapore.

[19] L. V. Tikhonov, V. A. Kononenko, G. I. Prokopenko *et al*., 1986. *Mechanical properties of metals and alloys.* Naukova Dumka, Kiev.

[20] H. Cyunn and C.-S. Yoo, 1999. Equation of state of tantalum to 174 GPa. *Physical Review B,* Vol. 59, p. 8526.

[21] M. J. Mahl and D. A. Papaconstantopoulos, 1996. Applications of a tight-binding total-energy method for transition and noble metals: Elastic constants, vacancies and surfaces of monatomic metals. *Physical Review B,* Vol. 54, No. 7, p. 4519.

[22] L.Vocadlo, G.D.Price and I. G. Wood, 1999. Crystal structure, compressibility and possible phase transitions in - FeSi studied by first-principles pseudopotential calculations. *Acta crystalographica Section B*, Vol. 55, pp. 484-493.

[23] R. Caracas and R.Wentzcovich, 2004. Equation of state and elasticity of FeSi. *Geophysical Research Letters,* Vol. 31, p. L20603.

[24] E. G. Moroni, W. Wolf, I. Hafner and R. Podloucky, 1999. Cohesive, structural and electronic properties of Fe-Si compounds. *Physical Review B,* Vol. 59, No. 20, p. 12860.

[25] D. P. Dobson, W. A. Crichton, P. P. Bouvier, L. Vocadlo and I. G. Wood, 2003. The equation of state of CsCl-structured FeSi to 40 GPa: Implications for silicon in the Earth's core. *Geophysical Research Letters,* Vol. 30, No. 1, p.14/1-4.